Available online at www.sciencedirect.com
SCIENCE DIRECT
Colloids and Surfaces A: Physicochem. Eng. Aspects 275 (2006) 92–98
COLLOIDS AND SURFACES A
www.elsevier.com/locate/colsurfa

Photoelectric conversion property of a photoresponsive D-π-A dye containing both N=N and CH=CH bonds

Fu-You Li [a,b], Yan-Yi Huang [c], Lin-Pei Jin [a,*], Jian-Quan Guo [a], Chun-Hui Huang [b,c,*]

[a] *Department of Chemistry, Beijing Normal University, Beijing 100875, PR China*
[b] *Laboratory of Advanced Materials, Fudan University, Shanghai 200433, China*
[c] *State Key Laboratory of Rare Earth Materials Chemistry and Applications, Peking University, Beijing 100871, PR China*

Received 21 May 2005; received in revised form 22 September 2005; accepted 23 September 2005
Available online 11 November 2005

Abstract

A new photoresponsive D-π-A dye, *N*-octadecyl-4-{2-[4-(2-(4-*N*,*N*-dimethylaminophenyl)azo)phenyl]ethenyl}pyridinium iodide (AEP) containing both CH=CH and N=N bonds, was synthesized, and *N*-octadecyl-4-[2-(4-*N*,*N*-dimethylaminophenyl)azo]pyridinium iodide (AP) and *N*-octadecyl-4-[2-(4-*N*,*N*-dimethylaminophenyl)ethenyl] pyridinium iodide (EP) were also synthesized for comparison. The photoelectric conversion (PEC) properties of the dye Langmuir–Blodgett (LB) monolayer films modified indium-tin oxide (ITO) electrode deposited under 20 mN m^{-1} of surface pressure were studied. The results show that AEP exhibits better PEC properties than AP and EP do. The photoelectric conversion efficiency is 0.31% for AEP in 0.5 mol L^{-1} KCl electrolyte solution under ambient condition, while those for AP and EP are 0.14 and 0.23% under the same conditions, respectively.

Keywords: Photoelectric conversion; LB films; Azobenzene derivative

1. Introduction

The potential application of organic thin films in nonlinear and electrooptics fields has attracted extensive research efforts for improving design and understanding of these thin films. Based on the reversibly photoinduced and thermally induced *cis–trans* isomerization of azobenzene, much attention was risen from azobenzene derivatives as functional compounds [1], because of their potential application to molecular devices, such as information storage system [2,3], nonlinear optics system [4–6] and photochemical switching systems [7,8]. In our previous publications, the azopyridinium dye *N*-octadecyl-4-[2-(4-*N*,*N*-dimethylaminophenyl)azo]pyridinium iodide (AP) (Scheme 1) [9] containing N=N bond exhibited photocurrent generation property. Then, we found that some hemicyanine dyes, such as *N*-octadecyl-4-[2-(4-*N*,*N*-dimethylaminophenyl)-ethenyl]pyridinium iodide (EP) (Scheme 1) [10] containing CH=CH bond, showed good photoelectric conversion (PEC) properties. How about the PEC property of a dye containing both CH=CH and N=N bonds is? Although the relation between the conjugation length of organic molecules and the nonlinear optical hyperpolarizability has been addressed [11], the conjugation dependence on photoelectric conversion property is not reported. Therefore, it is necessary to explore the PEC property of a new D-π-A dye by changing the π-conjugation bridge.

In this contribution, an amphiphilic azobenzene derivative, *N*-octadecyl-4-{2-[4-(2-(4-*N*,*N*-dimethylaminophenyl)-azo)phenyl]ethenyl}pyridinium iodide (AEP) (Scheme 1) was synthesized and successfully transferred onto quartz or indium-tin oxide (ITO) slides by Langmiur–Blodgett (LB) technique, and the photoelectric conversion properties of AEP LB monolayer films were investigated. For comparison, the PEC properties of the compounds AP and EP were also studied under the same conditions.

2. Experimental

4-Aminobenzaldehyde diazonium salt and 4-(4-*N*,*N*-dimethylaminophenyl)azo benzaldehyde were prepared according to the reported method [12]. The compound (AEP) was obtained as shown in Scheme 2 by condensation of

* Corresponding authors.

0927-7757/$ – see front matter © 2005 Elsevier B.V. All rights reserved.
doi:10.1016/j.colsurfa.2005.09.026

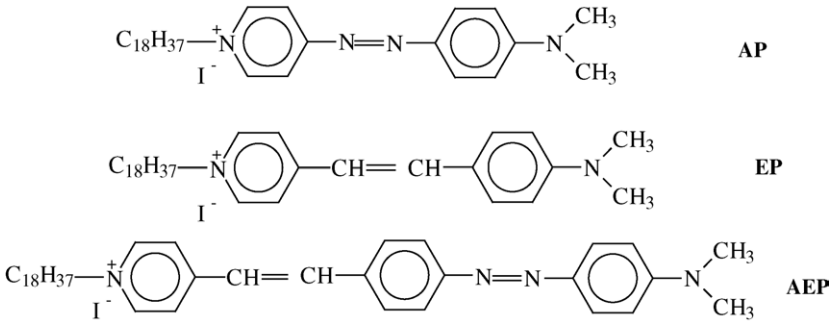

Scheme 1. Molecular structure of AP, EP and AEP dyes.

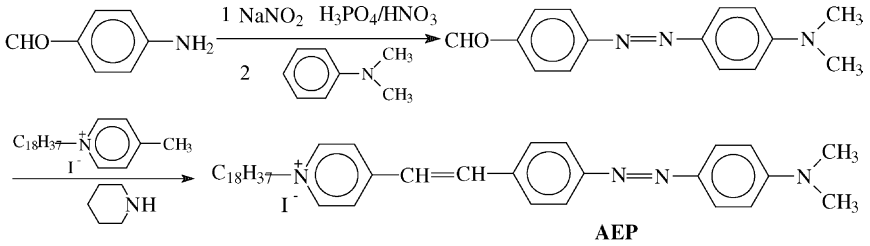

Scheme 2. The synthesis route of AEP dye.

N-octadecyl-4-methyl pyridinium iodide with an equivalent mole of 4-(4-dimethylaminophenyl)azo benzaldehyde in absolute ethanol using piperidine as the catalyst. The product was purified by column chromatography on silica gel with a chloroform–methanol mixture (15:1, v/v) as an eluent.

AEP: yield: 58%. m.p.: 212–214 °C. Anal. Calc. for $C_{39}H_{57}N_4I$: C, 67.20; H, 8.05; N, 7.81. Found: C, 67.00; H, 8.41; N, 7.38. δH (300 MHz, CDCl3): 0.87 (t, 3H, $1CH_3$), 1.24 (m, 30H, $15CH_2$), 1.85 (m, 2H, $1N^+$-CH_2CH_2), 3.10 (s, 6H, 2N-CH_3), 4.62(t, 2H, $1N^+$-CH_2), 6.72 (d, 2H, phenyl), 7.19 (d, 1H, CH=), 7.61 (d, 1H, CH=), 7.74 (d, 2H, phenyl), 7.85 (d, 2H, phenyl), 7.95 (m, 2H, phenyl), 8.11 (m, 2H, pyridyl), 8.91 (m, 2H, pyridyl).

The compounds *N*-octadecyl-4-[2-(4-*N*,*N*-dimethylaminophenyl) azo]pyridinium iodide (AP) [4] and *N*-octadecyl-4-[2-(4-*N*,*N*-dimethylaminophenyl)ethenyl]pyridinium iodide (EP) [13] were also synthesized for comparison. Methyl viologen diiodide (MV^{2+}) was synthesized by reaction of 4,4′-dipyridyl with methyl iodide. Its identity was confirmed by element analysis. The electrolyte for the electrochemical experiment was KCl (AR grade, Beijing Chemical Factory, China). Hydroquinone (H_2Q) (AR grade, Beijing Chemical Factory, China) was recrystallized from water before use. $EuCl_3.6H_2O$ was obtained by reaction of Eu_2O_3 with hydrochloric acid.

C, H, N data of the compounds were obtained by using a Carlo Erba 1106 elemental analyzer. ^{1}H NMR spectra were measured by using Bruker ARX300. Electronic spectra in solution or in LB films were recorded on a Shimadzu model 3100 UV–vis–Nir spectrophotometer. Melting point was performed on an X4 micromelting point apparatus.

A model 622 NIMA Langmuir–Blodgett trough was employed for the Langmuir–Blodgett study. Water obtained from an EASY pure RF system was used as the subphase ($R \sim 18\,M\Omega\,cm$, $pH \sim 5.6$). The substrates (ITO slide and quartz) were all hydrophilically pretreated as the previous methods [14]. A chloroform solution of $0.3\,mg\,mL^{-1}$ AEP dye (or AP and EP dye) was spread drop-by-drop from a chloroform-cleaned, glass microsyringe to the subphase surface ($20 \pm 1\,^\circ C$). After 15 min allowing the solvent to evaporate, the floating films were compressed at a ratio of $40\,cm^2\,min^{-1}$ and the surface pressure (π)–area (A) isotherms were recorded. For deposition of the first monolayer, the hydrophilic pretreated substrate was immersed in the subphase, then the monolayer was formed at the surface pressure of $20\,mN\,m^{-1}$ and transferred to solid substrate with a pulling rate of $5\,mm\,min^{-1}$. Only the films with transfer ratios of 1.0 ± 0.1 were used in the experiments. Here, transfer ratio is defined as the ratio of the area of monolayer removed from the water surface to the area of substrate coated by the monolayer. To ensure the formation of the hydrophilic surface, the ITO electrode was immersed for 2 days in a saturated methane solution of sodium methanoxide and then thoroughly rinsed with pure water under ultrasonication for several times.

Second harmonic generation (SHG) experiments were carried out with the laser beam (Nd:YAG, $\lambda = 1064\,nm$) at an angle of 45° to the LB monolayers. The SHG intensities were calibrated against a Y-cut quartz reference ($d_{11} = 0.5\,pm\,V^{-1}$). The data of second harmonic generation from the LB monolayer films were analyzed by general procedure described by Ashwell et al. [15].

Photoelectrochemical measurements were carried out in $0.5\,mol\,L^{-1}$ KCl aqueous solution using the dye LB monolayer film modified ITO electrode, platinum wire and saturated calomel electrode (SCE) as working electrode, counter electrode and reference electrode, respectively. Effective illuminated area of a flat window for AEP was $0.8\,cm^2$. The light source used for the photoelectrochemical study was a 500 W Xe arc lamp; the light beam passed through a group of filters (ca. 400–800 nm, Toshiba Co., Japan, and Schott Co., USA)

Table 1
Effect of solvent polarity on UV–vis spectra of AEP in solution

Solvent	Benzene	Chloroform	Dichloromethane	Pyridine	Ethanol	Methanol	Acetonitrile	DMSO
ε_{stat}	2.3	4.9	9.1	12.5	25.1	33.6	38.8	48.9
λ_{max} (nm)	498	500	499	489	576	475	474	472

Solvent static dielectric constants ε_{stat} (all quoted from Ref. [21]).

Table 2
The data of charge distribution at the different parts of molecules in the ground state and the excited state for AEP

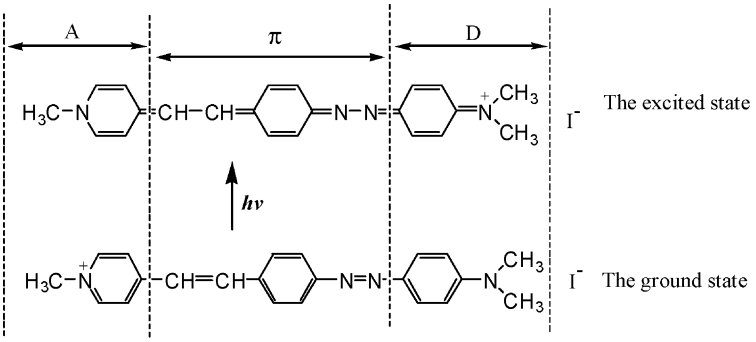

	A [a]	π [b]	D [c]	Σ [d]
The ground state	0.7967	0.0600	0.1433	0.6534
The excited state	0.3102	-0.0190	0.7088	-0.3986

	A^a	π^b	D^c	Σ^d
The ground state	0.7967	0.0600	0.1433	0.6534
The excited state	0.3102	−0.0190	0.7088	−0.3986

[a] Sum of the net charges of atoms at the acceptor part.
[b] Sum of the net charges of atoms at the π-conjugated bridge (CH═CH─phenyl─N═N).
[c] Sum of the net charges of atoms at the donor part.
[d] Symmetry deviation parameter $\Sigma = A - D$.

in order to get a given bandpass of light. The light intensity at each wavelength was measured with an energy and power meter (Scientech, USA). Cyclic voltammetry (CV) experiments (sweep rate = 100 mV S^{-1}) were performed on an EG&GPAR 273 potentiostat/galvanostat with EG&GPAR 270 electrochemical software in 0.5 mol L^{-1} KCl aqueous solution. Oxygen was removed from the electrolyte solution by bubbling N_2 before every measurement.

3. Results and discussion

3.1. Photophysical properties

The maximum wavelengths of absorption of AEP in various solvents are presented in Table 1. A large blue shift with increasing solvent polarity suggests that the AEP π–π^* transition is dramatically affected by the solvent polarity and the ground state has a larger solvation than the first excited single state does. It is concluded that the dipole of the ground state is larger than that of the excited state. Such experimental results were also confirmed by our theoretical calculations. Based on the assumption of neglecting the interactions of the molecules on the film, semiempirical quantum calculation was used to study the model molecule of AEP congener *N*-methyl-4-{2-[4-(2-(4-*N*,*N*-dimethylaminophenyl)azo)phenyl]ethenyl}pyridinium iodide (AEP′). First, the geometric structure of AEP′ is optimized by using the AM1 model Hamiltonian in the MOPAC 7.0 quantum chemical package [16]. Second, the charge distributions in the ground state and the excited state have been calculated by using MINDO/3 in MOPAC 7.0 method. The results of the calculation are given in Table 2. The symmetry deviation parameter $\sum$, defined as the sum of the π-charge densities on the half of the ethylene chain minus the sum of the π-charge densities on the other half [17], decreases from 0.6534 in the ground state to −0.3986 in the excited state in this system. Large decrease in the $\sum$ value in the excited state for AEP′ suggests an intramolecular electron (charge) transfer from the donor part (the dimethylanilino group) to the acceptor part (the pyridinium group) when the molecule is excited from the ground state to the excited state.

The surface pressure versus area isotherm of AEP is shown in Fig. 1, data show that the collapse pressure of AEP is 28.7 mN m^{-1}, and the limiting area per molecule of AEP is 0.81 nm^2, extrapolated the tangent of the π–*A* isotherm for AEP at 20 mN m^{-1}. For comparison, the data of AEP, AP and EP LB properties are illustrated in Table 3. It can be seen from

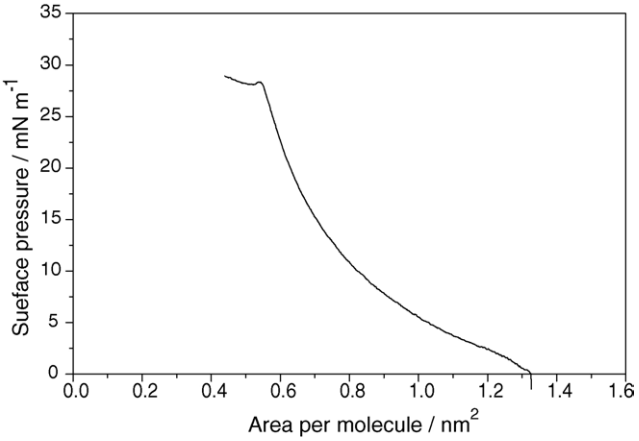

Fig. 1. Surface pressure–area (π–A) isotherm of AEP at the air/water interface ($20 \pm 1\,^{\circ}$C).

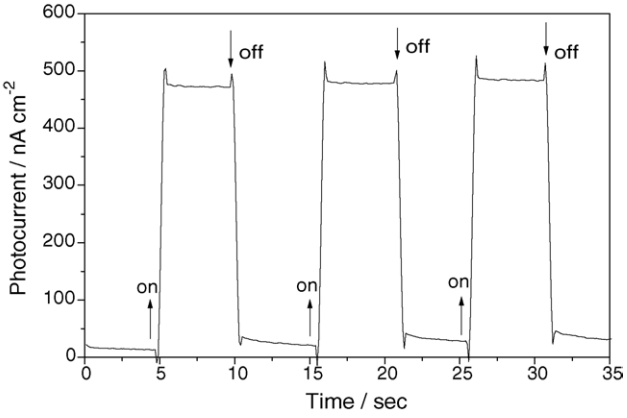

Fig. 2. The photocurrent generation response of AEP-ITO electrode in 0.5 mol L^{-1} KCl aqueous solution under ambient condition, upon irradiation of 137 mWcm^{-2} white light.

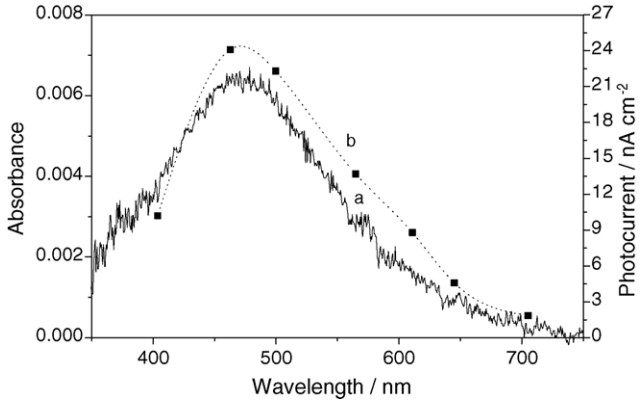

Fig. 3. UV–vis absorption spectrum (a) in LB monolayer films and action spectrum (b) of the cathodic photocurrent for AEP. The intensities of different wavelengths are all normalized.

Table 3 that the collapse pressure of AEP is lower than those of AP and EP, and that the molecular limiting area of AEP is larger than those of AP and EP. These differences are due to the different π-conjugated bridges for AP, EP and AEP, because their donor and acceptor groups are the same. The large molecular limiting area of AEP is due to its large π-conjugated bridge (–CH=CH–phenyl–N=N–). Moreover, the amphiphilic property in AEP is not very apparent, which causes the lower collapse pressure and larger molecular limiting area.

It can be seen from Table 3 that the maximum absorption wavelength moved from 500 nm in chloroform solution to 468 nm when it was fabricated on the ITO electrode. The larger blue shift results from the extended dipole interactions between the chromophores with small intermolecular separation distance, and indicates that H-aggregates formed in its LB monolayer films [18,19].

The second-order susceptibility $\chi^{(2)}$ of AEP LB monolayers deposited on quartz was 55 pm V^{-1}. Moreover, the result of SHG experiment showed that the tilt angle φ 51° of AEP LB monolayers deposited on quartz was larger than those of AP and EP LB monolayers (in Table 3), which supported the above conclusion of bigger molecular limiting area of AEP.

3.2. Photoelectric conversion properties (PEC)

A steady cathodic photocurrent was observed from AEP monolayer films modified ITO electrode in 0.5 mol L^{-1} KCl solution under illumination of 137 mW cm^{-2} white light. The photoelectric response remains stable when light is switched on and off (Fig. 2). The similarity of the action spectrum of the cathodic photocurrent to the absorption spectrum for AEP (see Fig. 3) indicates that the AEP LB monolayer films are responsible for photocurrent generation. The quantum yield (η) for the photocurrent generation was calculated according to the equations,

$$\eta = \frac{i}{[eI(1 - 10^{-A})]} \quad (1)$$

$$I = \frac{W\lambda}{hc} \quad (2)$$

where i is the observed photocurrent; e, the charge of the electron; I, the number of photons per unit area and unit time; A, the absorbance of the monolayer; λ, the wavelength of light irradiation; W, light power at λ nm; c, the light velocity; and h, the Planck constant. We obtained about 24.1 nA cm^{-2} of cathodic photocurrent and $\eta = 0.31\%$ (Table 4, η^{b}) for AEP LB monolayers under the zero bias voltage (versus SCE) at 464 nm (3.48×10^{15} photons $cm^{-2}\,s^{-1}$) in ambient condition, and the absorbance of the film was about 0.0060 at 464 nm.

Table 3
The data of AP, EP and AEP LB monolayer film properties

Dyes	P (mN m^{-1})	A (nm^2)	$\lambda_{max(film)}$ (nm)	$\lambda_{max(s)}$ (nm)	φ (°)
AEP	28.7	0.81	468	500	51
AP	50.6	0.50	550	560	40
EP	48.0	0.43	487	503	39

P: collapse pressure; A: molecular limiting area; $\lambda_{max(film)}$: absorption maximum on LB films; $\lambda_{max(s)}$: absorption maximum in chloroform solution. φ: tilt angle (relative to the normal line of the substrate).

Table 4
The photoelectric conversion properties of AP, EP and AEP dyes

Dyes	i[a] (nA cm^{-2})	No$_{(m)}$ (cm^{-2})	i'[a] (nA molecule^{-1})	i[b] (nA cm^{-2})	η[b] (%)	i[c] (nA cm^{-2})	η[c] (%)
AEP	475	1.23×10^{14}	3.86×10^{-12}	24.1	0.31	106	1.37
AP	394	2.00×10^{14}	1.97×10^{-12}	21.3	0.14	122	0.80
EP	552	2.33×10^{14}	2.37×10^{-12}	26.3	0.23	120	1.05

i: photocurrent per area; No$_{(m)}$: number of molecules per square centimeter; i': photocurrent per molecule; η: external quantum yield.
[a] Irradiation of 137 mW cm^{-2} white light for AEP, AP and EP, in 0.5 mol L^{-1} KCl electrolyte solution containing dissolved O_2.
[b] Irradiation of 137 mW cm^{-2} white light at 464, 550 and 464 nm for AEP, AP and EP, respectively, in 0.5 mol L^{-1} KCl electrolyte solution containing dissolved O_2.
[c] Irradiation of 137 mW cm^{-2} white light at 464, 550 and 464 nm for AEP, AP and EP, respectively, under −100 mV and in 0.5 mol L^{-1} KCl electrolyte solution containing dissolved O_2, 5 mM Eu^{3+} and 5.5 mM MV^{2+}.

3.3. Correlation between molecular structure and PEC property

To understand the relationship between the PEC property and the chemical structure, we chose 20 mN m^{-1} as the constant surface pressure for the dyes AEP, EP and AP in the deposited process. The data of photocurrent per square centimeter (Table 4, i) and external quantum yield (Table 4, η) apparently show that the PEC properties of AEP are better than those of AP and EP. Although the number of active moieties per unit area in the LB monolayers is an important factor contributing to the PEC performance, in these cases, the effects of chemical structural variations play the key role in resulting in the differences of the PEC properties for AEP, AP and EP. Taking the limiting molecular area into account, one can get the molecular numbers per square centimeter are 1.23×10^{14}, 2.00×10^{14} and 2.33×10^{14} for AEP, AP and EP (Table 4, No$_{(m)}$), respectively. Furthermore, with reference to the photocurrent per square centimeter, one can see that photocurrents per molecule of AEP, AP and EP are 3.86×10^{-12}, 1.97×10^{-12} and 2.37×10^{-12} nA molecule^{-1} (Table 4, i'), respectively. Apparently, AEP performs better in photocurrent generation than AP and EP do, which is mainly not due to the different number of molecules per square centimeter but due to the different chemical structure.

3.4. Dependence of PEC on experimental conditions

To explore the effect of bias voltage on photoinduced electron injection, the relationship between bias voltage and PEC property was investigated. Fig. 4 shows the dependence of photocurrent on bias voltage for AEP. The cathodic photocurrents for AEP increase as the negative bias voltage of the electrode rises, indicating that the photocurrent flows in the same direction as the applied negative voltage.

According to Donovan equation [20], the photocurrent (i_{ph}) has a dependence on light intensity (I), $i_{ph} = KI^m$, where $m = 1$ is the characteristic of unimolecular recombination and $m = 1/2$ is the characteristic of bimolecular recombination. The light intensity (I) dependence on the photocurrent (i_{ph}) measured at a zero bias potential for AEP LB monolayer films modified ITO electrode in 0.5 mol L^{-1} KCl electrolyte solution is shown in Fig. 5. The equation is $i_{ph} = 10.9I^{0.76}$ for AEP (see Fig. 5). Compared these equations with the generally used form, $i_{ph} = KI^m$, m is 0.76 for AEP, which indicates that the above two recombination processes occur in the LB monolayer film for AEP system simultaneously.

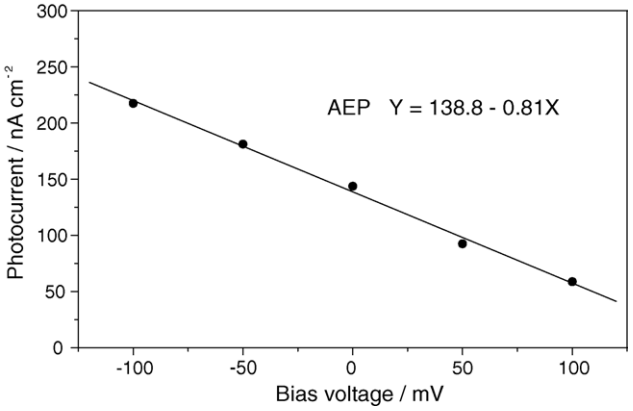

Fig. 4. Photocurrent versus bias voltage for AEP LB film-ITO electrode in 0.5 mol L^{-1} KCl aqueous solution under ambient condition, upon irradiation of 30.5 mW cm^{-2} white light.

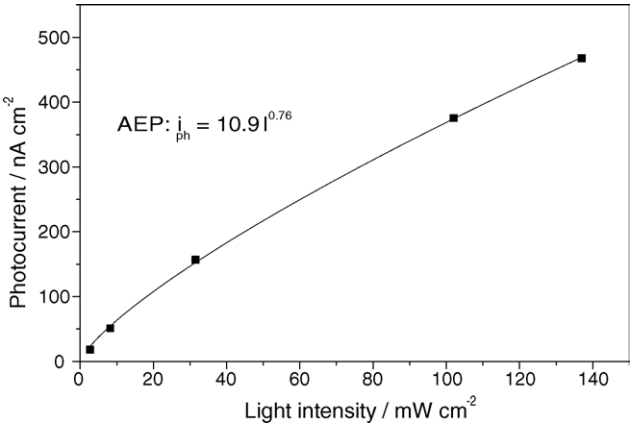

Fig. 5. Dependence of the photocurrent upon light intensity for AEP electrode in 0.5 mol L^{-1} KCl electrolyte solution under ambient condition without bias voltage.

It is well known that the intensity (even the direction) of photocurrent depends on the nature of the redox couple in the aqueous phase surrounding the electrode. The effects of electron donors and acceptors on the cathodic photocurrent for AEP show that electron acceptors (MV^{2+}, Eu^{3+} and O_2) sensitize the cathodic photocurrent and electron donors (H_2Q and N_2) quench it (even reverse it) (in Table 5). For example, it can be

Table 5
Effect of donors and acceptors on the photocurrent generation of AEP-ITO electrode

Donor/acceptor	Concentration (mM)	Photocurrent (nA cm^{-2})[a]		
		Ambient	N_2 degassed	O_2
MV^{2+}	0	158	55	182
	5.5	835	467	940
Eu^{3+}	0	165	59	190
	5	460	317	524
H_2Q	0	146	52	163
	4	−622[b]	−810[b]	−470[b]

[a] Irradiation under 30.5 mW cm^{-2} white light for AEP in 0.5 mol L^{-1} KCl solution.
[b] (−) stands for anodic photocurrent.

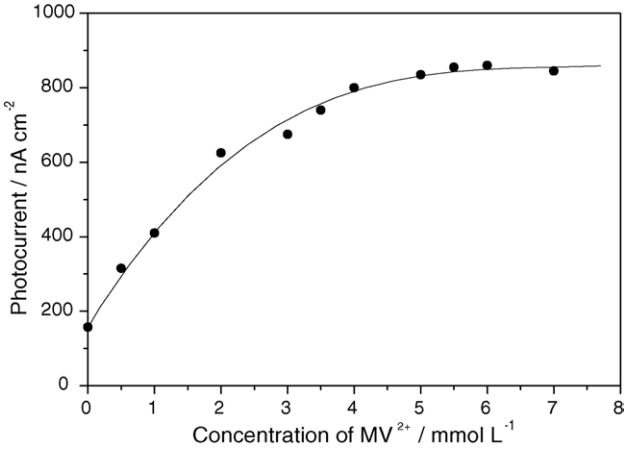

Fig. 6. Dependence of the photocurrent on the concentration of MV^{2+} under ambient condition for AEP monolayer upon irradiation with 30.5 mW cm^{-2} white light.

seen form Fig. 6 that the cathodic photocurrent increases gradually with increasing the concentration of MV^{2+} and starts to level off at 5.5 mmol L^{-1}. This means that MV^{2+} acts as an acceptor in accepting electrons from the AEP assemblies and therefore increases the concentration of electrons involved in the electron transfer process. Under favorable conditions, such as irradiation under 464 nm wavelength monochromized from 137 mW cm^{-2} white light and in the dissolved O_2 solution with 5 mmol L^{-1} Eu^{3+} and 5.5 mmol L^{-1} MV^{2+}, the photocurrent generation quantum yield for AEP is 1.37% (Table 4, η^c).

3.5. Mechanism of photoelectric conversion

The photochromic behavior originating from the *trans*- to *cis*-form occurs in the azobenzene compounds [21–23]. However, this phenomenon is generally suppressed or prohibited in LB membranes because of the lack of free space, which is due to the close packing of the azobenzene amphiphiles in the membranes. On the other hand, according to the Frank–Condon principle, the possibility for generating photocurrent under these circumstances is correlative with photoinduced electron transfer between the ITO substrate and excited-state dye within the LB monolayers. Here, we suggest that the photocurrent generation

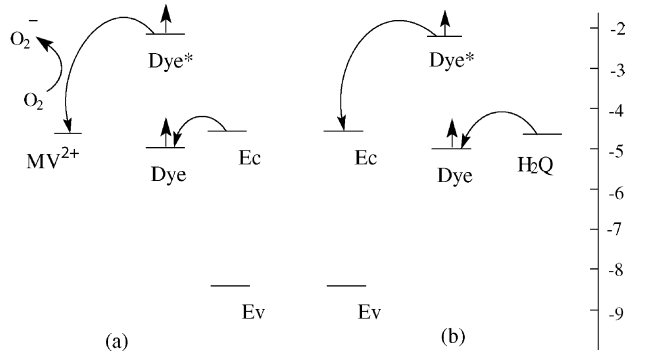

Scheme 3. The possible mechanism of the photoelectric conversion system of AEP: (a) cathodic photocurrent; (b) anodic photocurrent. (*) presents the excited state of the dye AEP.

of AEP is due to the photoinduced electron transfer and not to the photoisomerization of azobenzene unit.

To elucidate the mechanism of photoinduced electron transfer process for the cathodic and anodic photocurrent, the energy levels of the relevant electronic states should be estimated. Generally, the conduction band (Ec) and valence band (Ev) edges of the ITO electrode are estimated to be ca. −4.5 and −8.3 eV [24], respectively. Reduction potential of MV^{2+} is −4.51 eV (−0.23 V versus SCE) [25], and oxidation potential of H_2Q is −4.61 eV(−0.13 versus SCE) [25], on the absolute scale. The oxidation peak potential of a dye provides a measurement of the energy of the HOMO. The oxidation peak potential of 0.19 V from CV graph was observed for AEP LB monolayer film. Consequently, the energy level of the ground state for AEP LB monolayer film is −4.93 eV (0.19 V versus SCE) on the absolute scale. With reference to UV–vis spectrum of AEP LB monolayer film, the band gap between the ground state and excited state is 2.65 eV ($\lambda_{max(film)}$ = 468 nm) for AEP. Taking the energy level of the ground state and the band gap into account, the energy level of the excited state for AEP LB monolayer films is −2.18 eV on the absolute scale. Then, an energy level diagram for AEP is constructed as shown in Scheme 3, which describes the mechanism for photosensitization of the ITO electrode. In the presence of some electron acceptors, such as MV^{2+}, O_2 or Eu^{3+} in the electrolyte solution, electron transfers from the excited state of AEP to the electron acceptor, subsequently electron of ITO conduction band injects into the hole residing in the dye aggregate. Thus, cathodic photocurrent is generated. On the contrary, if there is a strong electron donor, such as H_2Q in the system, both ITO and H_2Q compete to donate an electron to the AEP LB monolayers, which will reduce cathodic photocurrent and even reverse the direction of photocurrent.

4. Conclusions

In conclusion, a new D-π-A dye containing both N=N and CH=CH bonds was synthesized and its photoelectrochemical properties were investigated. The results show that the photocurrent quantum yield (η) of the AEP system is higher than those of AP and EP containing corresponding N=N and CH=CH bond, respectively, which suggests that introduction of N=N bond into

D-π-A dye can improve the photocurrent generation property of the D-π-A dye. Therefore, the π-conjugation bridge is an important structure factor of PEC performance for organic D-π-A dye.

Acknowledgements

We thank the NHTRDP (863 Program No. 2002AA302403), the National Science Foundation of China (20490210) and Shanghai Sci.Tech. Comm. (03QB14006 and 03DZ12031) for financial support.

References

[1] J.A. Delaire, K. Natatani, Chem. Rev. 100 (2000) 1817.
[2] Z.F. Liu, K. Hashimoto, A. Fujishima, Nature 347 (1990) 658.
[3] T. Ikeda, O. Tsutsumi, Science 268 (1995) 1873.
[4] H. Li, D.J. Zhou, C.H. Huang, J.M. Xu, T.K. Li, X.S. Zhao, X.H. Xia, J. Chem. Soc., Faraday Trans. 92 (1996) 2085.
[5] Z. Sekkat, A. Knoesen, V.Y. Lee, R.D. Miller, J. Phys. Chem. B 101 (1997) 4733.
[6] H. Lei, H.Z. Wang, Z.C. Wei, X.J. Tang, L.Z. Wu, C.H. Tung, G.Y. Zhou, Chem. Phys. Lett. 333 (2001) 387.
[7] T. Ikeda, T. Sasaki, K. Ichimura, Nature 361 (1993) 428.
[8] B.L. Feringa (Ed.), Molecular Switches, Wiley-VCH, Weinheim, Germany, 2001.
[9] W.S. Xia, C.H. Huang, L.B. Gan, H. Li, J. Chem. Soc., Faraday Trans. 92 (1996) 3131.
[10] W.S. Xia, C.H. Huang, C.P. Luo, L.B. Gan, Z.D. Chen, J. Phys. Chem. 100 (1996) 15525.
[11] L.-T. Cheng, W. Tam, S.R. Marder, A.E. Stiegman, G. Rikken, C.W. Spangler, J. Phys. Chem. 95 (1991) 10643.
[12] M. Kawamura, T. Nishi, K. Kato, H. Mizokami, T. Kawazawa, Jpn. Kokai, Tokkyo. Koho. 41 (1979) 832, CA. 91, 107807Z.
[13] G.J. Ashwell, R.C. Hargreaves, C.E. Balduwin, G.S. Bahra, C.R. Brown, Nature 357 (1992) 221.
[14] D.G. Wu, C.H. Huang, L.B. Gan, Y.Y. Huang, Langmuir 14 (1998) 3783.
[15] G.J. Ashwell, P.D. Jackson, D. Lochum, W.A. Crossland, P.A. Thrompson, G.S. Bahra, C.R. Brown, C. Jasper, Proc. Roy. Soc. Lond. 445 (1994) 385.
[16] M. Utinans, O. Neilands, Adv. Mater. Opt. Electron. 9 (1999) 19.
[17] S. Dahne, Z. Chem. 21 (1981) 58.
[18] W.F. Mooney, P.E. Brown, J.C. Russell, S.B. Costa, L.G. Pedersen, D.G. Whitten, J. Am. Chem. Soc. 106 (1984) 5659.
[19] C.E. Evans, Q. Song, P.W. Bohn, J. Phys. Chem. 97 (1993) 12302.
[20] K.J. Donovan, R.V. Sudiwala, E.G. Wilson, Mol. Cryst. Liq. Cryst. 194 (1991) 337.
[21] H. Nakahara, K. Fukuda, M. Shimomura, T. Kuunitake, Nippon Kagaku Kaishi (1988) 1001.
[22] A. Yabe, Y. Kawabata, H. Niino, M. Tanaka, A. Ouchi, H. Takahashi, S. Tamura, W. Tagaki, H. Nakahara, K. Fukuda, Chem. Lett. (1988) 1.
[23] K. Nishiyama, M. Fujihira, Chem. Lett. (1988) 1257.
[24] L. Sereno, J.J. Silber, L. Otero, M.D.V. Bohorquez, A.L. Moore, T.A. Moore, D. Gust, J. Phys. Chem. 100 (1996) 814.
[25] Y.S. Kim, K. Liang, K.Y. Law, D.G. Whitten, J. Phys. Chem. 98 (1994) 984.